Acta Oceanol. Sin., 2020, Vol. 39, No. 7, P. 32–41
https://doi.org/10.1007/s13131-019-1627-8
http://www.hyxb.org.cn
E-mail: hyxbe@263.net

On the heat budget and water mass exchange in the Andaman Sea

Jiawen Liao[1, 4], Shiqiu Peng[1, 2, 3, 4*], Xixi Wen[1]

[1] State Key Laboratory of Tropical Oceanography, South China Sea Institute of Oceanology, Chinese Academy of Sciences, Guangzhou 510301, China

[2] Southern Marine Science and Engineering Guangdong Laboratory (Guangzhou), Guangzhou 511458, China

[3] Institution of South China Sea Ecology and Environmental Engineering, Chinese Academy of Sciences, Guangzhou, 510301 China

[4] University of Chinese Academy of Sciences, Beijing 100049, China

Received 24 February 2020; accepted 8 April 2020

Abstract

The characteristics of the T/S structures, water mass exchange and deep circulation in the Andaman Sea are investigated based on the simulation from a high-resolution general circulation model (MITgcm). The results show that, below 1 000 m, the water mass is saltier, warmer and more homogeneous in the Andaman Sea than that in the Bay of Bengal, attributing to the strong vertical mixing at the depth of ~1 800 m. The water mass exchange between the Andaman Sea and the Bay of Bengal goes through three major channels, which manifests itself as follows: the northern channel (Preparis Channel) is the main passage of water mass transport from the Bay of Bengal to the Andaman Sea, whereas the Middle Channel (the south of Andaman Islands and the north of Nicobar Islands) has an opposite transport; the southern channel (Great Channel) features with a four-layer water exchange which results in the least net transport among the three channels; all the transports through the three channels have an intra-annual variation with a period of half a year. At 1 000-m depth, the entire Andaman Sea is occupied by a cyclonic circulation in January and July while by an anticyclonic one in April and October. The semiannual cycle found in both the deep circulation and water mass exchange is likely associated with the downwelling eastward-propagating Kelvin waves induced by the semiannual westerly component in the equatorial Indian Ocean during intermonsoon seasons.

Key words: Andaman Sea, heat budget, water mass exchange, deep water circulation

Citation: Liao Jiawen, Peng Shiqiu, Wen Xixi. 2020. On the heat budget and water mass exchange in the Andaman Sea. Acta Oceanologica Sinica, 39(7): 32–41, doi: 10.1007/s13131-019-1627-8

1 Introduction

The Andaman Sea is a semi-enclosed marginal sea in the northeastern Indian Ocean, bounded by Myanmar on the north, Thailand and Malaysia on the east and the Andaman and Nicobar archipelagos on the west which separates the basin from the BOB (hereinafter denoted as BOB) (Fig. 1). It is connected to the BOB through three main channels: the Preparis Channel with a shallow depth of approximately 250 m, the Middle Channel including few passages between the south of Andaman islands and the north of Nicobar islands with a maximum depth of approximately 800 m, and the Great Channel with a maximum depth of approximately 1 800 m. The Andaman Sea is a completely isolated basin under 1 800 m whereas the water mass exchange is mainly through the Great Channel to the BOB and the equatorial Indian Ocean above 1 800 m.

The unique topography in the Andaman Sea provides ideal conditions for the formation of internal tides, which makes the Andaman Sea one of the most energetic tidal regions in the world (Niwa and Hibiya, 2011; Mohanty et al., 2018). Meanwhile, as a part of the Indian monsoon area, the Andaman Sea is dominated by southwest winds in the summer and northeast winds in the winter, with transition periods in spring and autumn (De Boyer Montégut et al., 2004). In addition, the summer monsoon precipitation in this region is the highest summer rainfall in the Indian Ocean (Qi and Wang, 2015). The large amount of rainfall together with large runoff from the Irrawaddy result in significantly low surface salinity with the strong stratification of the surface layer (Sprintall and Tomczak, 1992). Moreover, the Andaman Sea is a crucial pathway of Kelvin waves propagating from the equatorial Indian Ocean to the Bay of Bengal (Chatterjee et al., 2017).

Previous studies of the Andaman Sea were mainly based on the limited observations. Kiran (2017) attempted to fully describe the dynamics of Andaman Sea surface circulation from observations. The circulation in Andaman Sea is characterized by gyres or vortices, which is the manifestation of Rossby waves of semi-annual mode (Kiran, 2017). Liu et al. (2018) studied the sea-

Foundation item: The National Natural Science Foundation of China under contract Nos 41931182, 41521005 and 41676016; Guangdong Key Project under contract No. 2019BT2H594; the Key Special Project for Introduced Talents Team of Southern Marine Science and Engineering Guangdong Laboratory (Guangzhou) under contract Nos GML2019ZD0303 and GML2019ZD0304; the Chinese Academy of Sciences under contract Nos ZDRW-XH-2019-2 and ISEE2018PY05; the Independent Research Project Program of State Key Laboratory of Tropical Oceanography under contract Nos LTOZZ1902 and LTOZZ1802.
*Corresponding author, E-mail: speng@scsio.ac.cn

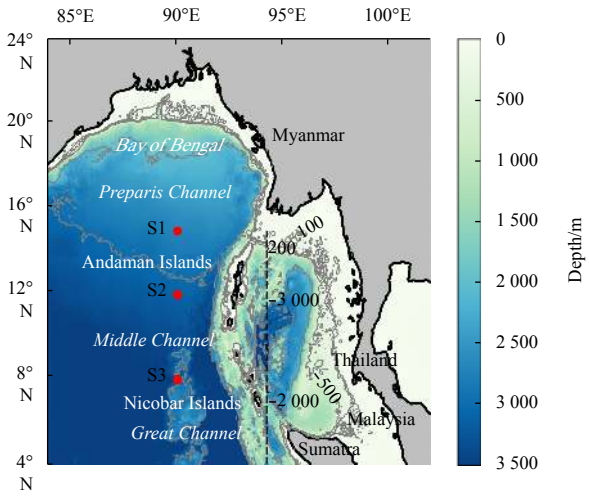

Fig. 1. The model domain and the bathymetry (units: m) of the Andaman Sea. The red dots denote the locations of the *in-situ* observations from RAMA moorings and the black dashed line denotes the section along 94.2°E for the analyses in Figs 6a and 7.

sonal variations of the upper ocean structure and the air-sea interactions in the central Andaman Sea using a moored surface buoy. They found that the net surface heat fluxes dominated the seasonal double peak pattern of the sea surface temperature and the surface water is warmer in the winter in Andaman Sea than that in the BOB because of less heat loss. SenGupta et al. (1981) and Sarma and Narvekar (2001) had given observational evidences of large differences in the water mass properties, including physical and biogeochemical variables between the Andaman Sea and the BOB. Dutta et al. (2007) measured the physical and chemical properties of the water mass at two sites in the Andaman Sea basin and the results were in good agreement with the previous studies from SenGupta et al. (1981) and Sarma and Narvekar (2001). Their observations indicated that the physical and chemical properties of the Andaman Sea vary very little below 1 300-m depth. Okubo (2004) used the vertical distribution of ^{230}Th to estimate the renewal time of the deep water mass in the Andaman Sea is about 6 years based on a two-dimensional scavenging-mixing model. Due to the limitation of observations, the fundamental physical characteristics in the deep Andaman Sea have not been fully documented. Chatterjee et al. (2017) first studied the dynamical processes of the Andaman Sea based on a numerical model. Their results suggest that the coastal circulation within the Andaman Sea and around the islands is primarily driven by equatorial forcing and the local wind forcing. However, their study only focused on the upper layer (200-m and 575-m depth) of the Andaman Sea, leaving the circulation in the deep Andaman Sea an open issue. Thus, this study attempts to address this issue by using a high-resolution general circulation model, focusing on the water mass properties and deep-water circulation in the Andaman Sea, as well as the water mass exchange with the BOB through the three channels.

This paper is organized as follows. A short description of the model and data is given in Section 2. In Section 3, model results are evaluated against observations and reanalysis data. Section 4 presents the analysis based on the model results. A summary with a short discussion is given in Section 5.

2 Model and data

The Massachusetts Institute of Technology General Circulation Model (MITgcm; Marshall et al., 1997), formulated in z coordinates, is used in the present study. The model domain extends from 4°–24°N and 84°–102°E with a horizontal resolution of (1/12)°×(1/12)°, covering the entire Andaman Sea and part of the Bay of Bengal (Fig. 1). There are 58 layers in the vertical with nonuniform thickness increasing from the surface (10 m) to the bottom (100 m).

The mixing parameterization is set as follows: The horizontal and vertical eddy viscosities are calculated using the Leith scheme (Leith, 1996) and the subgrid-scale vertical mixing processes are parameterized by the K-Profile parameterization (KPP) scheme (Large et al., 1994), respectively. The horizontal and vertical background diffusivities are set to 500 m^2/s and 1×10^{-5} m^2/s, respectively. Due to the strong interaction between tides and the topography, the KL10 scheme (Klymak et al., 2010) is used in the model to parameterize the process of internal tidal mixing near the bottom boundary. The Gent-McWilliams/Redi (GMRedi) subgrid-scale eddy parameterization is adopted to eliminate spurious diapycnal mixing by orienting the diffusion tensor into the isopycnal and diapycnal directions (Redi, 1982) and adiabatically rearranges tracers through an advective flux (Gent and McWilliams, 1990; Gent et al., 1995).

The model topography is taken from the General Bathymetric Chart of the Oceans (GEBCO14) bathymetry data (http://www.gebco.net) with a high resolution of 30 arcs. The model is forced by 10-m winds, 2-m air temperature, shortwave radiation and longwave radiation, which are interpolated from National Centers for Environmental Prediction (NCEP) CRV2 climatology data. Sensible and latent heat fluxes are calculated online using the bulk formula. The initial and boundary temperature and salinity are derived from the Generalized Digital Environmental Model, version 3 (GDEMv3) (http://www.usgodae.org/pub/outgoing/static/ocn/gdem/). The initial and boundary velocities are derived from the Simple Ocean Data Assimilation (SODA) 3.6.1 climatology data. Meanwhile, the model is forced by eight tidal constituents (M_2, S_2, K_1, O_1, N_2, K_2, P_1 and Q_1) at the open boundaries. The amplitudes and phases are extracted from the Oregon State University (OSU) inverse barotropic tidal model (OTIS) (Egbert et al., 1994; Egbert and Erofeeva, 2002) with 1/30° spatial resolution (http://volkov.oce.orst.edu/tides/YS.html). Furthermore, an additional sponge layer is applied at the southern and eastern open boundaries of the model domain to reduce artificial reflection. In order to prevent temperature and salinity from drifting, sea surface temperature and salinity are relaxed to the monthly mean GDEMv3 climatology with a time scale of 30 days. The model is integrated forward for 50 years, and the results of the final 10 years are selected for the analyses in this paper.

The observational dataset World Ocean Atlas 2013 (WOA13) is used to validate the model temperature and salinity, while two reanalysis datasets, Simple Ocean Data Assimilation (SODA) 3.6.1 and Estimating the Circulation and Climate of the Ocean (ECCO2), are used for comparison. WOA13 is a climatological mean dataset of oceanographic variables including the temperature and salinity based on in-situ measurements gridded into a horizontal resolution of (1/4)°×(1/4)° and 102 vertical levels. SODA 3.6.1 is an ocean reanalysis dataset consisting of gridded variables for the global ocean with a horizontal resolution of (1/2)°×(1/2)° and 50 vertical levels. ECCO2 is a monthly-averaged product with a horizontal resolution of (1/4)°×(1/4)° and 50 vertical levels. The T/S *in-situ* observations from the three moorings of Research Moored Array for African-Asian-Australian Monsoon Analysis (RAMA) (8°N, 12°N and 15°N) at 90°E (Fig. 1) for 12 years (2008–2019) are monthly averaged to obtain the cli-

matological mean.

3 Model validation

Figure 2 shows the cross-section distributions of the biases for potential temperature and salinity along 10°N for the deep layer (>500 m) against WOA13 for SODA3.6.1, ECCO2 and our model simulation (here after referred to as MITgcm SIML), respectively. In the BOB, the biases of both the potential temperature and salinity are tiny for SODA3.6.1, ECCO2 and MITgcm SIML. In the Andaman Sea, however, large deviation in either the potential temperature or salinity is seen in SODA3.6.1 and ECCO2 with the biases of 1–2°C and 0.025–0.100 psu respectively, whereas the deviations are much smaller for MITgcm SIML with biases of only about 0.4°C and 0.010 psu respectively.

The T/S profiles in the BOB from RAMA moorings are compared with those from the MITgcm SIML, as shown in Fig. 3. Due to the limitation of observations, the temperature and salinity validation are made only above 550-m depth and 150-m depth, respectively. The largest deviations of modeled temperature and salinity are respectively 2–3°C and 1 psu from the observations at the thermocline about 80–100 m depth. Wind stress has effects on the Ekman pumping and the horizontal transport of seawater, further affecting the change of thermocline (Miller et al., 1997; Wang et al., 1999; Liu et al., 2000). However, the variability of the climatological wind used in the model is too weak to reproduce the depth of thermocline accurately, which results in large deviations of temperature and salinity near the thermocline. Below the 100-m depth, the modeled and observed temperature in these sites are in good agreement with each other. Since the deep water mass properties are well reproduced by the model, it is believed that the properties of the deep circulation in the Andaman Sea captured by the model, which are in lack of observations currently, are somehow reliable.

4 Results and discussion

4.1 *Properties of water mass*

The cross-sections of potential temperature and salinity in the Andaman Sea and the BOB along 10°N, 95°E and 90°E are shown in Fig. 4. The deep-water properties in the Andaman Sea are in dramatically contrast to those in the BOB below 1 000 m (Figs 4a and b); the sea water in the Andaman Sea is saltier, warmer and more vertically uniform below 1 000 m than that in the BOB. In the Andaman Sea (Figs 4c and d), the potential temperature and the salinity near the bottom are about 4.4°C and 34.86 psu, whereas in the BOB (Figs 4e and f) they are about 1.7°C and 34.75 psu.

To figure out the mechanism responsible for the contrast between the two basins, a heat budget analysis is performed below 1 000 m over the entire Andaman Sea and BOB basins based on the following equation, respectively:

$$\underbrace{\frac{\partial T}{\partial t}}_{\text{temperature tendency}} = \underbrace{-\boldsymbol{u}\cdot\nabla T}_{\text{advection}} + \underbrace{\nabla_H(\kappa_H\nabla_H T) + \frac{\partial}{\partial z}\left(\kappa_z\frac{\partial T}{\partial z}\right)}_{\text{diffusion}}, \quad (1)$$

where T is the potential temperature, $\partial T/\partial t$ is the temperature tendency, $\boldsymbol{u}$ is the velocity vector, ∇ is the three-dimensional gradient operator, κ_H and κ_z are the horizontal and vertical diffusivities, respectively. The right-hand side of Eq. (1) includes the advection and diffusion that contribute to the temperature tendency. All terms are output from the MITgcm online diagnostics. Hence, the discretization of the budget is exactly the same as the model formulations and the budget equation should be exactly closed (i.e., the temperature tendency in the left-hand side equals the sum of the terms in the right-hand side).

The averaged heat budget below 1 000 m depth in the Andaman Sea and the BOB are shown in the Fig. 5. It can be seen that the curves of the temperature tendency directly output from the model and that computed as a sum of all the terms in the right-hand side of Eq. (1) are completely overlapped for both the Andaman Sea and the BOB, indicating that Eq. (1) is exactly closed. Above 1 800 m depth (Figs 5a and b), the temperature tendency nearly overlap with those of the advection and the change of the temperature are dominant by the process of advection in the Andaman Sea and the BOB. Below 1 800 m depth (Figs 5c and d), the advection and the diffusion play different roles in the Andaman Sea and the BOB. In the BOB, the effect of diffusion becomes more prominent than that above 1 800 m and advection still plays a dominant role in the increasing or decreasing of the temperature. However, in the Andaman Sea, the diffusion term plays a vital role in the heat balance by increasing the deep-water temperature, while the advection term contributes to the decreasing of the deep-water temperature. The variation of the diffusion term is associated with that of the advection term, because the

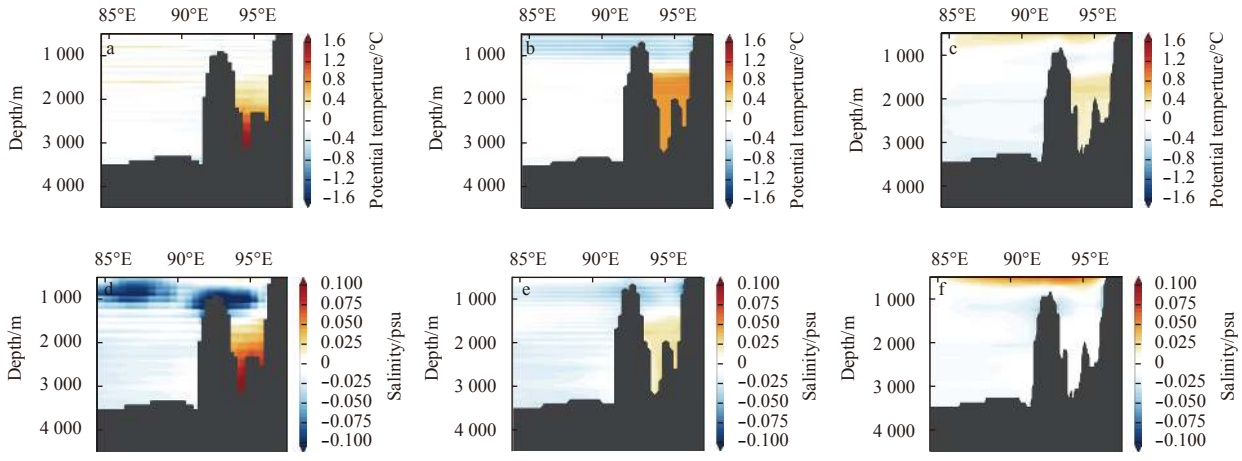

Fig. 2. Cross-section distributions of the differences in potential temperature (°C) (top) and salinity (psu) (bottom) between WOA dataset and SODA3.6.1 (a, d), ECCO2 (b, e), as well as MITgcm SIML(c, f) along 10°N, respectively.

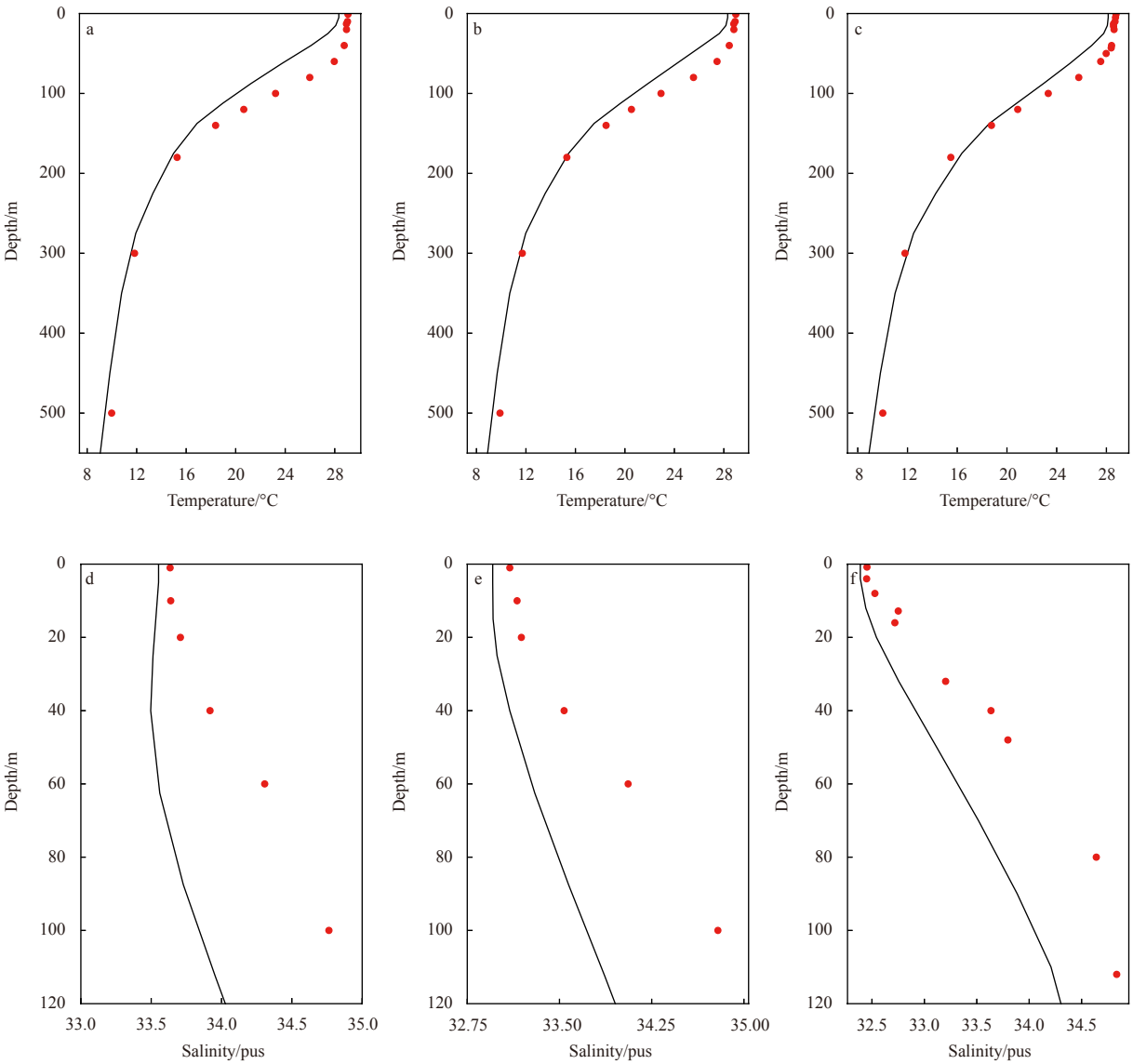

Fig. 3. The profile of temperature (top) and salinity (bottom) from the model (black line) and the RAMA observations (red point) in the S1 (a, d) , S2 (b, e) as well as S3 (c, f). The locations of these sites are shown in Fig. 1.

cold water advection changes the stratification which influences the strength of the vertical mixing.

Figure 6a shows the cross-section distribution of the potential temperature along 94.2°E. There is a dramatic contrast in the temperature between BOB and the Andaman Sea. The cross-section distribution of the annual mean velocity across the Great

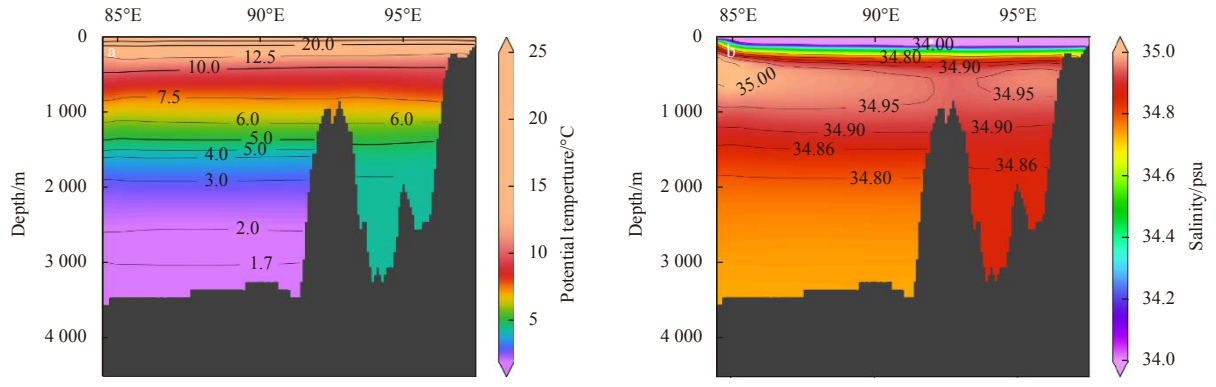

Fig. 4.

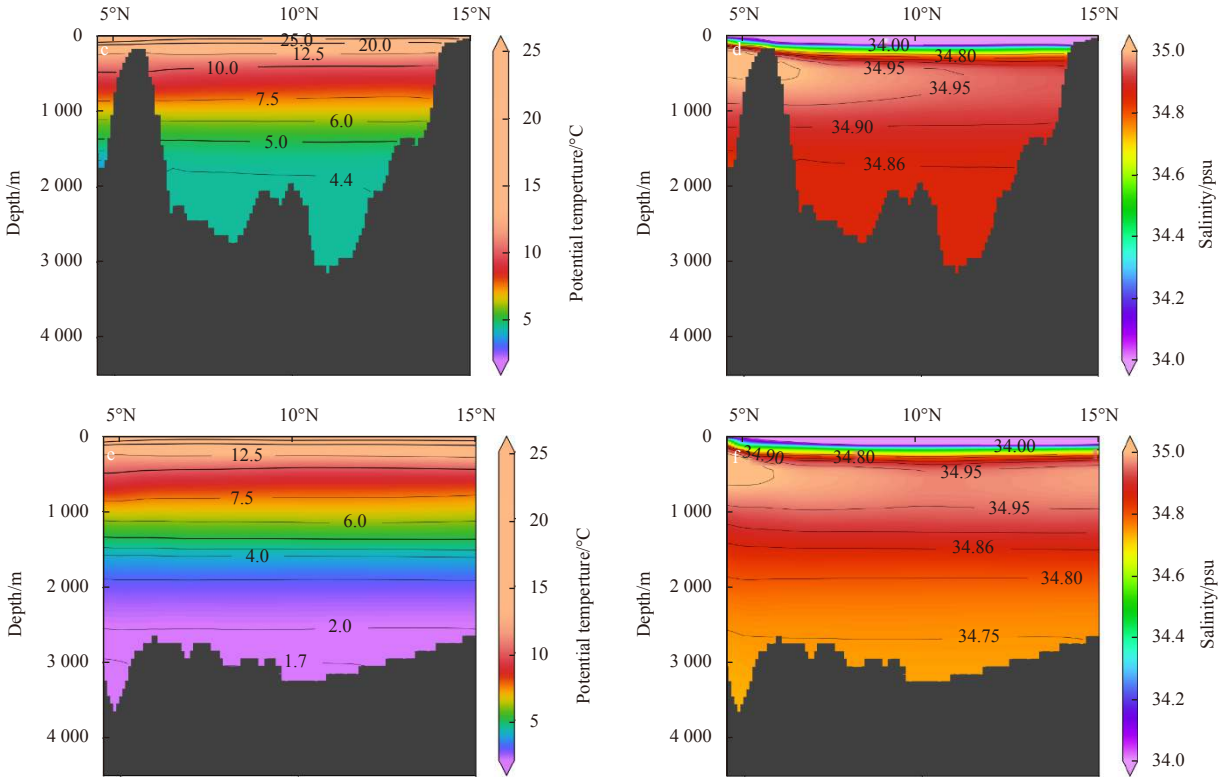

Fig. 4. Cross-section distributions of potential temperature (°C) (a, c, e) and salinity (psu) (b, d, f) along 10°N (a, b), 95°E (c, d) and 90°E (e, f).

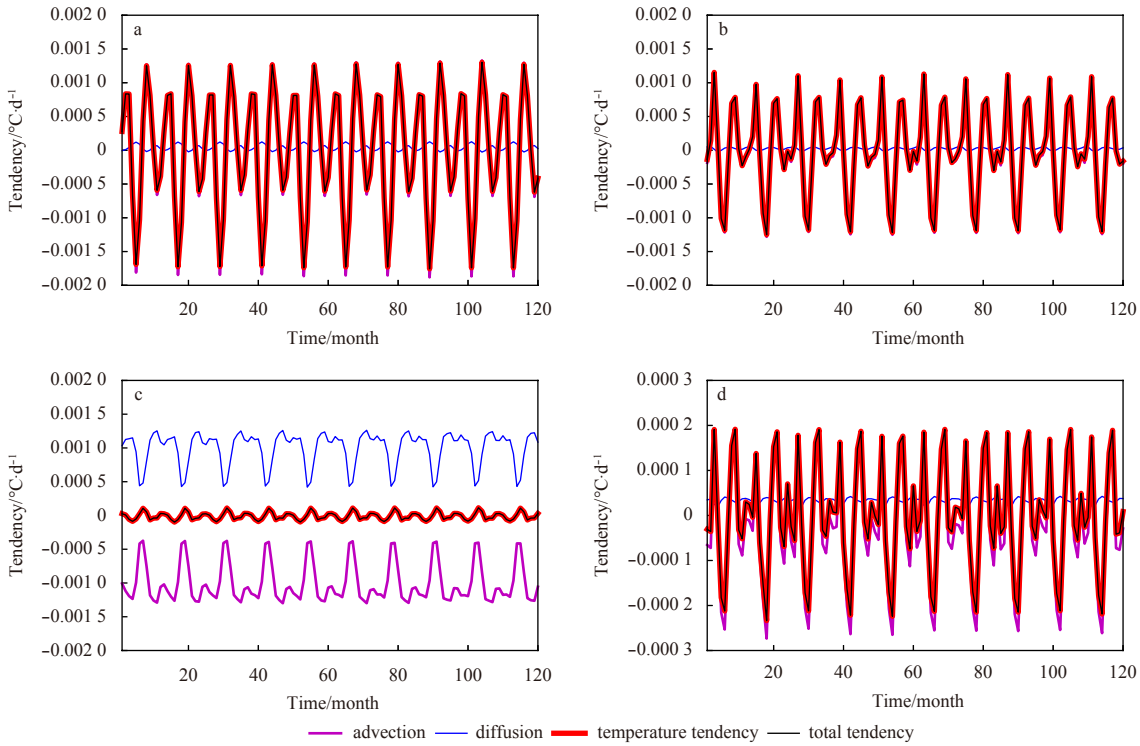

Fig. 5. The averaged heat budget includes total tendency, advection, as well as diffusion terms from 1 000 m depth to 1 800 m depth(a, b) and below 1 800 m depth (c, d) in the Andaman Sea (a, c) and the BOB (b, d). The term of the total tendency is a sum of all the terms on the right-hand side of Eq. (1).

Channel is shown in Fig. 6b. The positive (negative) value indicates the inflow (outflow) from the BOB (Andaman Sea) to the Andaman Sea (BOB). Near the bottom of the channel (~about 1 800 m), there is a strong inflow with colder water from the BOB to the Andaman Sea; Andaman Sea gets replenishment of fresher and colder water from the BOB at this depth.

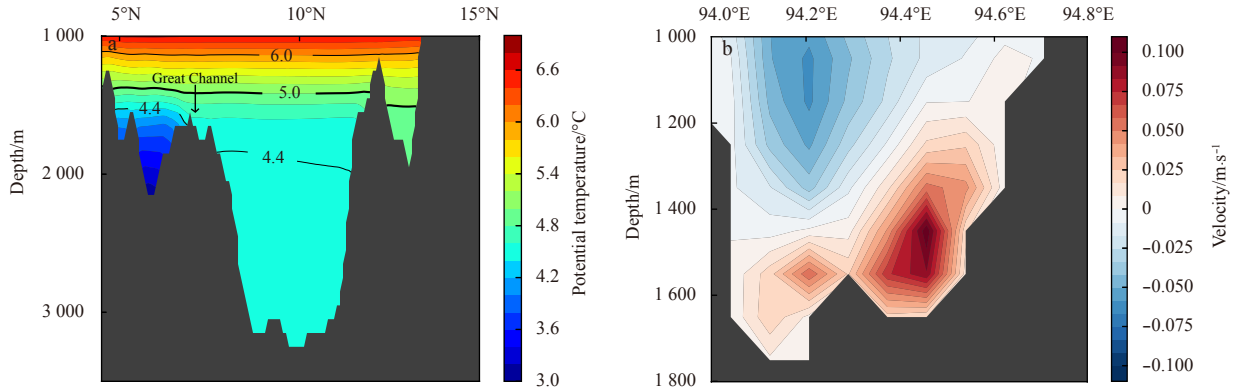

Fig. 6. Cross-section distributions of the potential temperature along 94.2°E (a) (seen as Fig. 1) and the annual mean normal velocity (m/s along the Great Channel (b). The positive value denotes the inflow from the BOB to the Andaman Sea, while the negative value is opposite.

Figure 7 shows the cross-section distributions of vertical diffusivity along 94.2 °E. Enhanced mixing with vertical diffusivity of $O(10^{-3}–10^{-1})$ m^2/s occurs at 1 800 m in the Andaman Sea that is the depth of the fresh water replenished from the BOB to the Andaman Sea, which is about 1–3 orders of magnitude larger than that in the BOB. The enhanced mixing near 1 800 m in the Andaman Sea could counter the cooling effect of the advection to keep the contrast between these two basins.

4.2 *Water mass exchange*

The normal transports across the sections of these three channels are calculated, and positive sign means the transport from the BOB to the Andaman Sea and vice versa. The profiles of transports in the three main channels between the BOB and the Andaman Sea as well as the net transport are shown in Fig. 8 and Table 1. For the Preparis Channel, the transport is relatively large and always inward (indicating by positive value of transport) from the BOB to the Andaman Sea in January and July with a net transport of 1.36×10^6 m^3/s and 1.45×10^6 m^3/s, respectively, whereas in the April and October, the water transport is weak and changes direction at 50 m depth, with the net transport of about -0.15×10^6 m^3/s and -0.05×10^6 m^3/s, respectively. In the annual mean, the net transport (~0.64×10^6 m^3/s) is an inward flow from the BOB to the Andaman Sea. For the Middle Channel, the annu-

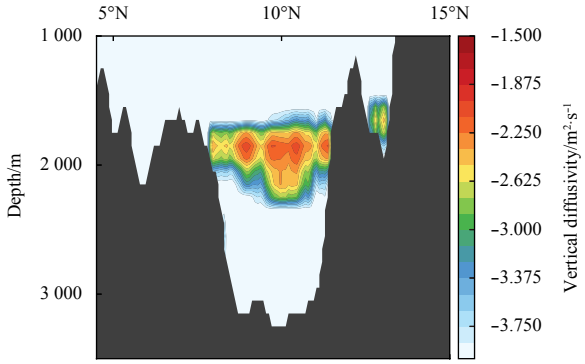

Fig. 7. Cross-section distribution of the logarithm ($\log_{10}$) of vertical diffusivity (m^2/s) along 94.2°E (seen as Fig. 1).

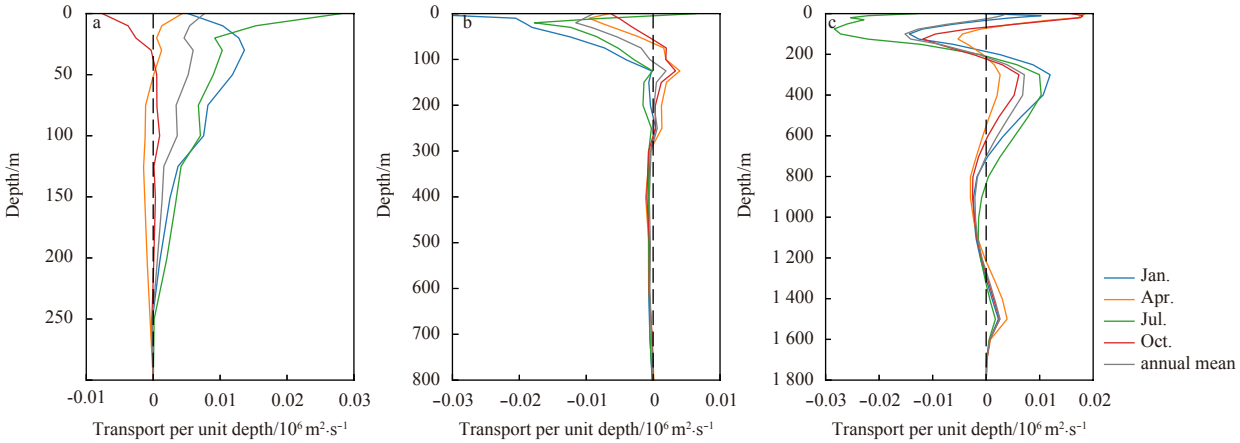

Fig. 8. Transport profile (10^6 m^2/s) for Preparis Channel (a), Middle Channel (b) and Great Channel (c) in January (blue), April (orange), July (green), October (red) and annual mean (grey). The positive value denotes the inflow from the BOB to the Andaman Sea, while the negative value is opposite.

Table 1. The net transport (unit: 10^6 m^3/s) of three main channels in January, April, July and October

Channel	January	April	July	October	Annual mean
Preparis Channel	1.36	–0.15	1.45	–0.05	0.64
Middle Channel	–1.77	–0.29	–1.25	–0.25	–0.68
Great Channel	1.85	0.54	–0.44	0.49	0.29

Note: The positive value denotes the inflow from the BOB to the Andaman Sea, while the negative value is opposite.

al mean transport (~–0.68 × 10^6 m^3/s) is opposite to the Preparis Channel, i.e., toward the BOB. In January and July, the transport is toward the BOB from the surface to the bottom with a larger net transport of about –1.77×10^6 m^3/s and –1.25×10^6 m^3/s, respectively, while the transport in April and October is toward the BOB above (below) 50 m (300 m) depth and toward the Andaman Sea between 50 m and 300 m depths, resulting in a smaller net transport of about –0.29 × 10^6 m^3/s and –0.25×10^6 m^3/s.

The Great Channel is the main passage linking the Andaman Sea to the BOB. Its vertical transport structure is significantly different from the other two passages and is thus more complicated. The transport shows a four-layer water exchange centered at the depths of about 100 m, 300 m, 1 000 m and 1 500 m, respectively. There is an outflow from the Andaman Sea to the BOB above 250 m depth, while an inflow from 250 m to 750 m depths occurs. Between 750 m and 1 300 m depths, the transport orientation turns toward the BOB again, while there is a weak inflow to the Andaman Sea at the bottom of the passage. While the vertically-integrated transport is toward the Andaman Sea from the BOB and the equatorial Indian Ocean in January, April and October with an estimation of 1.85×10^6 m^3/s, 0.54×10^6 m^3/s and 0.49×10^6 m^3/s, respectively, it is outward the Andaman Sea in July with an estimation of –0.44×10^6 m^3/s. In the annual mean, the total net transport in the Great Channel is about 0.29×10^6 m^3/s from the BOB to the Andaman Sea. Although the Great Channel is the deepest passage linking the Andaman Sea and the BoB, its annual mean net volume transport is the least among the three channels.

Figure 9 shows the temporal variations of the monthly mean net transport in three channels. A semiannual variation is roughly seen in the Preparis Channel (the Middle Channel) with peeks (toughs) in May (April) and November (October), while an annual variation appears in the Great Channel with peak in the winter and trough in in summer. In order to further investigate the annual or semiannual variations of the net transport in these three channels, the 10-year series of the net transport are analyzed using the power spectrum, which is shown in the Fig. 10. In the surface layer, there is a prominent annual-cycle signal in all of the three channels (Figs 10a, b and c), which is associated with the annual-cycle of local winds (Kiran, 2017). However, there is a prominent semi-annual cycle below the Ekman layers for all the channels (Figs 10d, e and f) and these results are similar with the studies from Potemra et al. (1991), which could be related to semi-annual cycle of the eastward-propagating Kelvin waves in the equatorial Indian Ocean and will be discussed in the last section.

4.3 *Deep circulation*

The deep-water circulation at the 1 000 m depth in the Andaman Sea is shown in Fig. 11. In January and July, the basin is dominant by a cyclonic circulation centered at about 10.5°N and 94°E where is the deepest water depth (>3 000 m) in the basin (Fig. 1). The circulation reverses to anticyclonic in the April and October, suggesting a semiannual cycle similar to that of the water mass exchange through the three channels. Enhanced southward (northward) branch of the cyclonic (anticyclonic) circulation at the western boundary occurs with a maximum velocity of

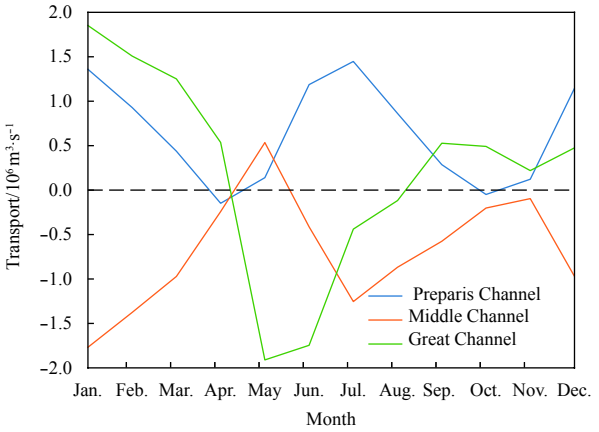

Fig. 9. Temporal variations of the monthly mean net transport in the three channels. The positive value denotes the inflow from the BOB to the Andaman Sea, while the negative value is opposite.

0.045 m/s (0.08 m/s) in July (April), while the relatively weak but broad northward (southward) branch is seen in the middle of the basin with a maximum velocity of 0.02 m/s (0.03 m/s) in July (April). In addition, there is a southward flow along the eastern slope of the basin in January and July, which is intensified in the southern portion of the slope with a maximum velocity of 0.045 m/s in July. At 1 000 m depth, the water mass exchange between the Andaman Sea and the BOB can only occur through the Great Channel, which manifests a year-round outward flow from the BOB to the Andaman Sea; the outward flow is stronger in the northern portion of the channel and in the monsoon transition seasons with maximum velocity of 0.12 m/s in April.

Figure 12 shows the vertical section of the zonal velocity along 95°E in January, April, July and October, respectively. Above 1 500 m, the deep circulation in the Andaman Sea presents a significant signal of semiannual cycle. Westward flow occurs in the north and south of the basin with the maximum velocity of 0.043 m/s in January and July. There is an eastward flow in the middle of this basin in January and July, and the maximum of the velocity is up to 0.014 m/s in July. In April and October, opposite situation occurs; westward flow occurs in the middle of the basin with maximum velocity of 0.024 m/s in April, while the eastward flow occurs in the north and south of the basin with the maximum velocity of 0.104 m/s and 0.079 m/s in April and October, respectively. Below 1 500 m, due to the similar structure of temperature and salinity, the vertical distribution of zonal velocity has no significant seasonal change.

5 Discussionand summary

This study analyzes the climatological water mass properties and deep ocean circulation in the Andaman Sea based on a simulation using MITgcm. The results reveal that: (1) There is a dramatic contrast in temperature and salinity between the Andaman Sea and the BOB. The sea water in the Andaman Sea is warm-

er, saltier and much less stratified than the BOB below 1 000 m depth. There is the strong vertical mixing to counter the advection near the 1 800 m depth contributing to the decreasing of the temperature and keep the heat balance in the Andaman Sea, which could be the reason maintaining the different vertical T/S structures in the two regions. (2) The Preparis Channel is the one with the largest net volume transport from the BOB to the Andaman Sea with an annual mean transport of 0.64×10^6 m^3/s, where-

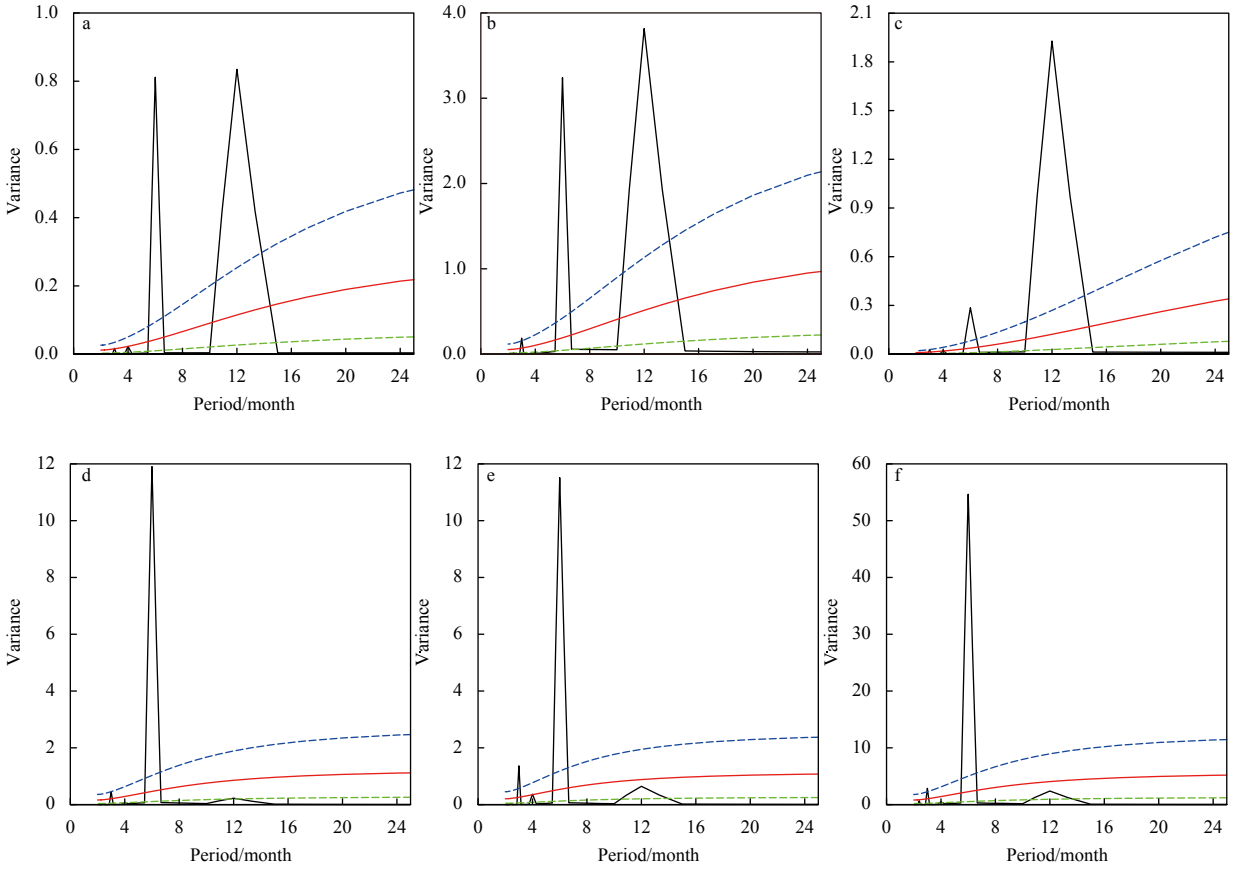

Fig. 10. Power spectrum analysis for the water exchange in the Preparis Channel (a, d), the Middle Channel (b, e), and the Great Channel(c, f) on the surface layer (a, b, c) and below the Ekman layer (d, e, f). The red curves represent the red noise. The blue one and the green one indicate the upper (95%) and the lower (5%) confidence bounds.

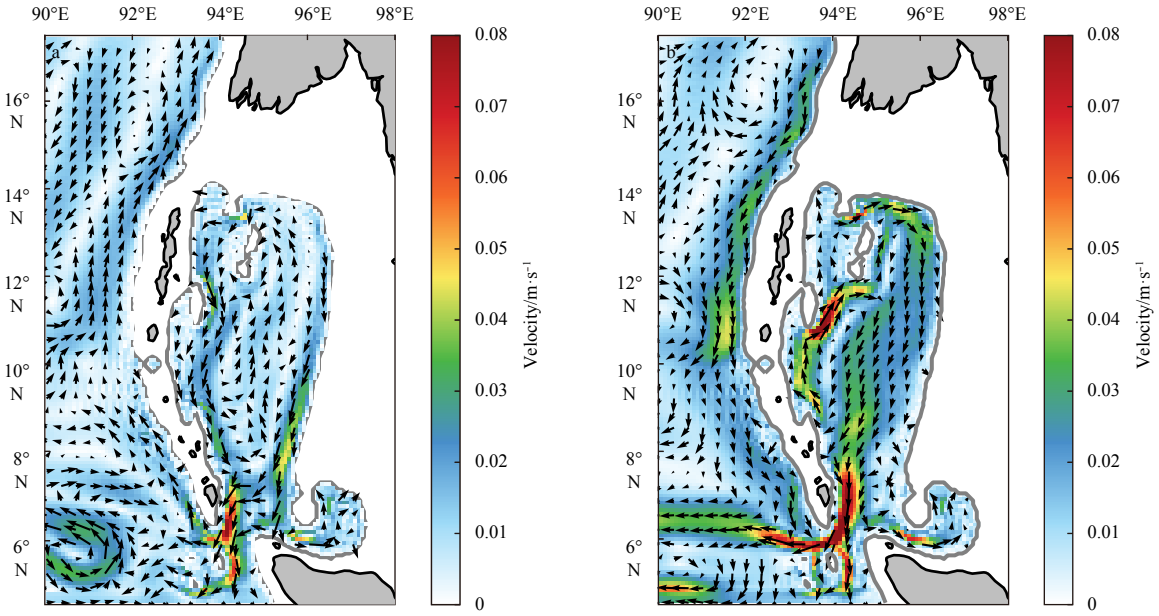

Fig. 11.

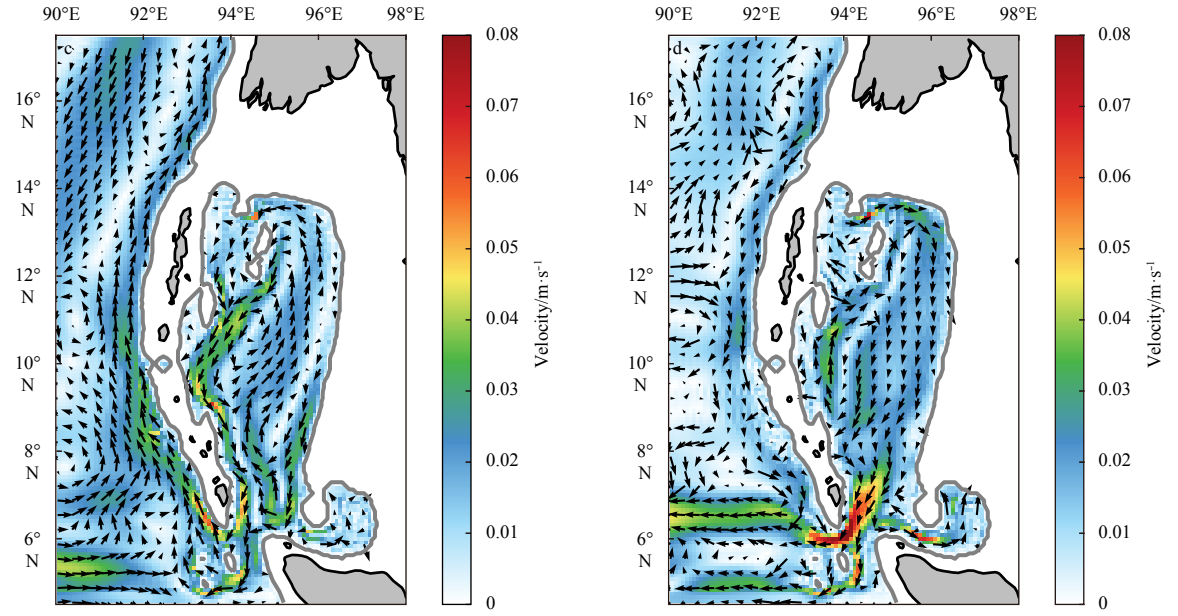

Fig. 11. The deep ocean circulation at the 1 000 meters in the Andaman Sea in January (a), April (b), July (c), and October (d). The shading is the magnitude of velocity.

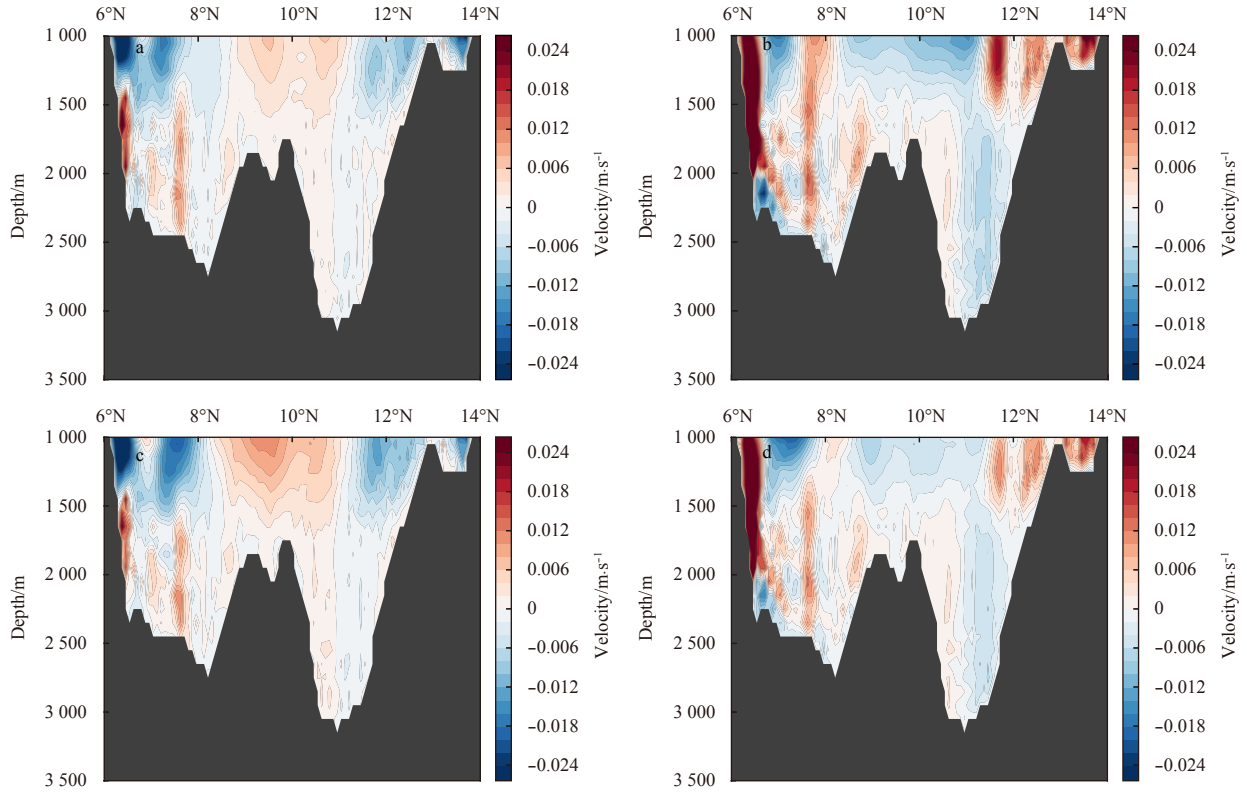

Fig. 12. Vertical profile of the zonal velocity (m/s) along 95°E in January (a), April (b), July(c) and October (d).

as the Middle Channel is the one with the largest net volume transport from the Andaman Sea to the BOB with an annual mean transport of 0.68×10^6 m^3/s. Meanwhile, the Great Channel shows a complex four-layer vertical structure of inward and outward water exchange with an annual mean transport of 0.29×10^6 m^3/s from the BOB to the Andaman Sea. (3) The water mass exchange and the deep circulation in the Andaman Sea present a significant signal of semiannual cycle. The cyclonic circulation at 1 000 m depth dominates during monsoon seasons, while it reverses to an anticyclonic one during the intermonsoon seasons. The southward (northward) western boundary currents of the cyclonic (anticyclonic) circulation are intensified with the speed up to 0.08 m/s in April.

It is worth noting that the semi-annual variability in the water

mass exchange between the two basins through the three channels and the deep ocean circulation in the Andaman Sea may be associated with the eastward-propagating Kelvin waves in the equatorial Indian Ocean. During the monsoon-transition periods (April–May and October–November), westerly winds prevail in the central and eastern Indian Ocean, generating energetic eastward equatorial currents, commonly known as Wyrtki Jets (Wyrtki, 1973; Nagura and McPhaden, 2010), as well as downwelling equatorial Kelvin waves. The Kelvin waves propagate eastward from the wind-forced region and reflect as a packet of coastally trapped Kelvin waves at the coast of Sumatra (Chatterjee et al., 2017). The reflected waves propagate along the eastern boundary, across the interior of the Andaman Sea, and eventually have impacts on the circulation in the interior of the Andaman Sea (Potemra et al., 1991; McCreary et al., 1993, 1996; Vinayachandran et al., 1996). The dynamical mechanism influencing the deep circulation in the Andaman Sea is still unclear and worth our further investigation in the future. Finally, since the results of the water mass exchange and deep circulation in the Andaman Sea presented in this study are mainly based on model simulation, in-situ observations in that region are definitely in demand to verify these results.

References

Chatterjee A, Shankar D, McCreary J P, et al. 2017. Dynamics of Andaman Sea circulation and its role in connecting the equatorial Indian Ocean to the Bay of Bengal. Journal of Geophysical Research: Oceans, 122(4): 3200–3218, doi: 10.1002/2016JC012300

De Boyer Montégut C, Madec G, Fischer A S, et al. 2004. Mixed layer depth over the global ocean: An examination of profile data and a profile-based climatology. Journal of Geophysical Research: Oceans, 109(C12): C12003, doi: 10.1029/2004JC002378

Dutta K, Bhushan R, Somayajulu B L K. 2007. Rapid vertical mixing rates in deep waters of the Andaman Basin. Science of the Total Environment, 384(1–3): 401–408, doi: 10.1016/j.scitotenv.2007.04.041

Egbert G D, Bennett A F, Foreman M G G. 1994. TOPEX/POSEIDON tides estimated using a global inverse model. Journal of Geophysical Research: Oceans, 99(C12): 24821–24852, doi: 10.1029/94JC01894

Egbert G D, Erofeeva S Y. 2002. Efficient inverse modeling of barotropic ocean tides. Journal of Atmospheric and Oceanic Technology, 19(2): 183–204, doi: 10.1175/1520-0426(2002)019<0183:EIMOBO>2.0.CO;2

Gent P R, McWilliams J C. 1990. Isopycnal mixing in ocean circulation models. Journal of Physical Oceanography, 20(1): 150–155, doi: 10.1175/1520-0485(1990)020<0150:IMIOCM>2.0.CO;2

Gent P R, Willebrand J, McDougall T J, et al. 1995. Parameterizing eddy-induced tracer transports in ocean circulation models. Journal of Physical Oceanography, 25(4): 463–474, doi: 10.1175/1520-0485(1995)025<0463:PEITTI>2.0.CO;2

Kiran S R. 2017. General circulation and principal wave modes in Andaman Sea from observations. Indian Journal of Science and Technology, 10(24): doi: 10.17485/ijst/2017/v10i24/115764

Klymak J M, Legg S, Pinkel R. 2010. A simple parameterization of turbulent tidal mixing near supercritical topography. Journal of Physical Oceanography, 40(9): 2059–2074, doi: 10.1175/2010JPO4396.1

Large W G, McWilliams J C, Doney S C. 1994. Oceanic vertical mixing: a review and a model with a nonlocal boundary layer parameterization. Reviews of Geophysics, 32(4): 363–403, doi: 10.1029/94RG01872

Leith C E. 1996. Stochastic models of chaotic systems. Physica D: Nonlinear Phenomena, 98(2–4): 481–491, doi: 10.1016/0167-2789(96)00107-8

Liu Yanliang, Li Kuiping, Ning Chunlin, et al. 2018. Observed seasonal variations of the upper ocean structure and air-sea interactions in the Andaman Sea. Journal of Geophysical Research: Oceans, 123(2): 922–938, doi: 10.1002/2017JC013367

Liu Qinyu, Yang Haijun, Wang Qi. 2000. Dynamic characteristics of seasonal thermocline in the deep sea region of the South China Sea. Chinese Journal of Oceanology and Limnology, 18(2): 104–109, doi: 10.1007/BF02842568

Marshall J, Adcroft A, Hill C, et al. 1997. A finite-volume, incompressible Navier Stokes model for studies of the ocean on parallel computers. Journal of Geophysical Research: Oceans, 102(C3): 5753–5766, doi: 10.1029/96JC02775

McCreary J P, Han W, Shankar D, et al. 1996. Dynamics of the east India coastal current: 2. numerical solutions. Journal of Geophysical Research: Oceans, 101(C6): 13993–14010, doi: 10.1029/96JC00560

McCreary J P, Kundu P K, Molinari R L. 1993. A numerical investigation of dynamics, thermodynamics and mixed-layer processes in the Indian Ocean. Progress in Oceanography, 31(3): 181–244, doi: 10.1016/0079-6611(93)90002-U

Miller A J, White W B, Cayan D R. 1997. North Pacific thermocline variations on ENSO timescales. Journal of Physical Oceanography, 27(9): 2023–2039, doi: 10.1175/1520-0485(1997)027<2023:NPTVOE>2.0.CO;2

Mohanty S, Rao A D, Latha G. 2018. Energetics of semidiurnal internal tides in the Andaman Sea. Journal of Geophysical Research: Oceans, 123(9): 6224–6240, doi: 10.1029/2018JC013852

Nagura M, McPhaden M J. 2010. Wyrtki jet dynamics: seasonal variability. Journal of Geophysical Research: Oceans, 115(C7): C07009

Niwa Y, Hibiya T. 2011. Estimation of baroclinic tide energy available for deep ocean mixing based on three-dimensional global numerical simulations. Journal of Oceanography, 67(4): 493–502, doi: 10.1007/s10872-011-0052-1

Okubo A, Obata H, Nozaki Y, et al. 2004. ^{230}Th in the Andaman Sea: Rapid deep-sea renewal. Geophysical Research Letters, 31(22): doi: 10.1029/2004GL020226

Potemra J T, Luther M E, O'Brien J J. 1991. The seasonal circulation of the upper ocean in the Bay of Bengal. Journal of Geophysical Research: Oceans, 96(C7): 12667–12683, doi: 10.1029/91JC01045

Qi Li, Wang Yuqing. 2015. Discrepancies in different precipitation data products in the Bay of Bengal during summer monsoon season. Advances in Meteorology, 2015, 806845

Redi M H. 1982. Oceanic isopycnal mixing by coordinate rotation. Journal of Physical Oceanography, 12(10): 1154–1158, doi: 10.1175/1520-0485(1982)012<1154:OIMBCR>2.0.CO;2

Sarma V V S S, Narvekar P V. 2001. A study on inorganic carbon components in the Andaman Sea during the post monsoon season. Oceanologica Acta, 24(2): 125–134, doi: 10.1016/S0399-1784(00)01133-6

SenGupta R, Moraes C, George M D, et al. 1981. Chemistry and hydrography of the Andaman Sea. Indian Journal of Marine Sciences, 10(3): 228–233

Sprintall J, Tomczak M. 1992. Evidence of the barrier layer in the surface layer of the tropics. Journal of Geophysical Research: Oceans, 97(C5): 7305–7316, doi: 10.1029/92JC00407

Vinayachandran P N, Shetye S R, Sengupta D, et al. 1996. Forcing mechanisms of the Bay of Bengal circulation. Current Science, 71(10): 753–763

Wang Bin, Wu Renguang, Lukas R. 1999. Roles of the western North Pacific wind variation in thermocline adjustment and ENSO phase transition. Journal of the Meteorological Society of Japan, Ser. II, 77(1): 1–16, doi: 10.2151/jmsj1965.77.1_1

Wyrtki K. 1973. An equatorial jet in the Indian Ocean. Science, 181(4096): 262–264, doi: 10.1126/science.181.4096.262